Measurement of thin film magnetostriction using field-dependent atomic force microscopy

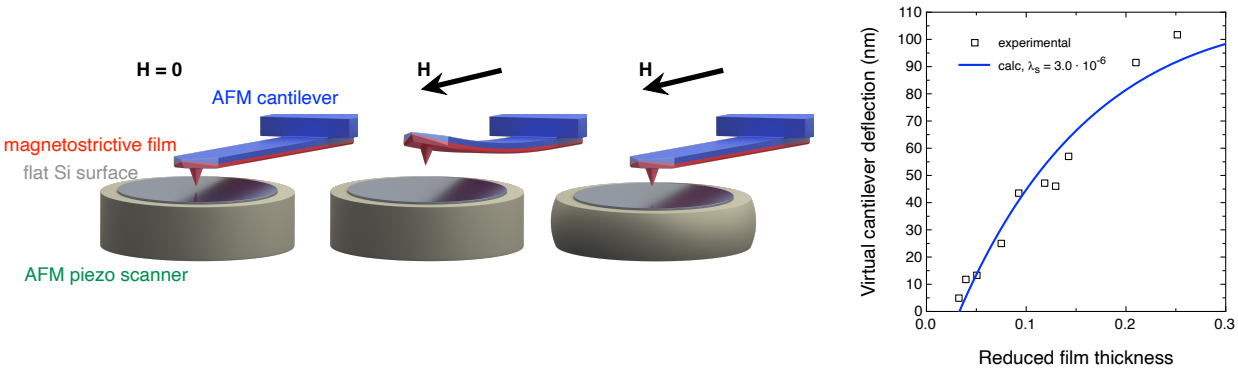

An AFM cantilever coated with a magnetostrictive film constitutes a bimorph reacting to an applied magnetic field. Attractive interactions between the cantilever tip and a flat surface, of adhesion and capillary origin, allow the AFM to react and keep the cantilever deflection constant by displacing the piezoelectric scanner. A suitable model of the forces acting on the cantilever allows to extract the magnetostriction constant of the coating film.

Measurement of thin film magnetostriction using field-dependent atomic force microscopy

Marco Coïsson[1], Wilhelm Hüttenes[2], Matteo Cialone[3,1], Gabriele Barrera[1], Federica Celegato[1], Paola Rizzi[3], Zoe H. Barber[2], Paola Tiberto[1]

[1] Advanced Materials and Life Sciences Division, INRIM, Torino, Italy
[2] Department of Materials Science and Metallurgy, Cambridge University, UK
[3] Department of Chemistry, University of Torino, Italy

Corresponding authors who equally contributed to the research:

Marco Coïsson, m.coisson@inrim.it
Wilhelm Hüttenes, wkgh2@cam.ac.uk

Abstract

Measurement of thin film magnetostriction is a challenging task, as magnetostrictive material deformations in parts per million, in conjunction with materials at small dimensions, require high precision, often with dedicated set-ups, for reproducible results. We have developed a novel approach employing a commercial atomic force microscope (AFM) with attached electromagnets. Magnetostriction measurements are demonstrated on 50 – 500 nm thick $Fe_{81}Al_{19}$ films sputter deposited directly on high aspect ratio commercial AFM micro-cantilevers. A magnetostrictive deflection of the cantilever bimorph translates into a deflection force acting in a contact mode measurement, which is interpreted and recorded as a change in height. For determination of the magnetostriction coefficient λ_s, we have developed a modified version of the equation for the magnetostrictive deflection of a cantilever bimorph by Guerrero and Wetherhold, taking into account long-range attractive forces acting during contact mode AFM measurements in air. The sub-atomic precision of the AFM, combined with the widespread availability of all components and the simple set-up, makes the measurement of magnetostriction on films of just a few tens of nanometers thickness easily accessible.

Keywords

Magnetostriction; thin films; atomic force microscopy; Fe-Al; cantilever method

Measurement of thin film magnetostriction using field-dependent atomic force microscopy

Marco Coïsson[1],* Wilhelm Hüttenes[2],† Matteo Cialone[3,1], Gabriele Barrera[1], Federica Celegato[1], Paola Rizzi[3], Zoe H. Barber[2], and Paola Tiberto[1]

[1] *Advanced Materials and Life Sciences Division, INRIM, Torino, Italy*

[2] *Department of Materials Science and Metallurgy, Cambridge University, UK and*

[3] *Department of Chemistry, University of Torino, Italy*

* m.coisson@inrim.it

† wkgh2@cam.ac.uk

ABSTRACT

Measurement of thin film magnetostriction is a challenging task, as magnetostrictive material deformations in parts per million, in conjunction with materials at small dimensions, require high precision, often with dedicated set-ups, for reproducible results. We have developed a novel approach employing a commercial atomic force microscope (AFM) with attached electromagnets. Magnetostriction measurements are demonstrated on $50 - 500$ nm thick $Fe_{81}Al_{19}$ films sputter deposited directly on high aspect ratio commercial AFM micro-cantilevers. A magnetostrictive deflection of the cantilever bimorph translates into a deflection force acting in a contact mode measurement, which is interpreted and recorded as a change in height. For determination of the magnetostriction coefficient λ_s, we have developed a modified version of the equation for the magnetostrictive deflection of a cantilever bimorph by Guerrero and Wetherhold, taking into account long-range attractive forces acting during contact mode AFM measurements in air. The sub-atomic precision of the AFM, combined with the widespread availability of all components and the simple set-up, makes the measurement of magnetostriction on films of just a few tens of nanometers thickness easily accessible.

I. INTRODUCTION

Given their capability to couple electromagnetic and mechanical energy, magnetostrictive materials, whose dimensions change under the application of a magnetic field [1], can be fundamental building blocks for transducers, MEMS and NEMS [2, 3], wirelessly controlled actuators [4], sensors [5, 6], nanomechanical systems for mass and force detection of molecules and atoms in biomedicine [7–15], and in solid state physics [16–18]. A variety of methods has been exploited to measure magnetostriction, which is in the order of a few tens to thousands of parts per million, including strain gauges [1, 19], tunnelling tip dilatometers [1], small-angle magnetisation rotation [20–22], and strain and ferromagnetic resonance methods [20, 23]. For thin film samples dimension variations become very small, and carefully tailored techniques are required to amplify the deformation of the magnetostrictive material [24]. Among these, cantilever-based systems are the most versatile, allowing reproducible and reliable detection by, principally, capacitive methods [20, 25] and optical means,

such as fiber optic dilatometers [20], interferometers [26], and laser optics [27–29]. A significant drawback of these approaches is, however, the requirement for a dedicated and often custom-made setup, as well as specific sample preparation. A promising alternative to this is atomic force microscopy (AFM), being an established and widespread method with the capability to detect sub-nanometric features. Early studies have employed conventional AFM imaging for magnetostriction measurements on metallic wires [30, 31]. More recently, it has successfully been demonstrated for thin film magnetostriction by measuring the tip deflection of micromachined macro-cantilevers (a few millimetres to centimetres in size), coated with Fe, Ni, Co and Tb based magnetostrictive films [32, 33]. In a related approach for dynamic force microscopy in liquid environments, the AFM probes (with micro-cantilevers a few μm in size) have been directly coated with 50 nm films of magnetostrictive Fe-B-N, to drive their mechanical oscillation [34].

In this work, we have taken these approaches further by developing a thin film magnetostriction measurement method employing AFM micro-cantilevers in an unmodified atomic force microscope, equipped with an electromagnet for application of magnetic fields. Commercial, mechanically soft AFM cantilevers are directly coated with $50-500$ nm thick magnetostrictive $Fe_{81}Al_{19}$ films by sputter deposition. During a contact-mode experiment on a very small, flat area a varying homogeneous magnetic field is applied along the cantilever length. This enables a measurement of the magnetostrictive force exerted by the deflection of the bimorph (magnetic film on cantilever) with precise field resolution, giving a full deflection *vs.* field curve as a result. This technique avoids any need for custom apparatus or preparation of special cantilevers, using only commercial components, while extracting the best from the capability of atomic force microscopes to measure size variations at sub-nanometric resolution, with the highest sensitivity derived from the use of micro-cantilevers. Its potential to analyse any magnetostrictive material that can be deposited or grown by physical or chemical methods to coat AFM cantilevers renders it similarly versatile to conventional cantilever-based methods. While the deflection force of the bimorph is directly measured by the atomic force microscope, the calculation of the magnetostriction constant of the magnetic material is indirect. Existing mathematical expressions for the deflection of such bimorphs based on the early works by du Trémolet *et al.* [35] do not fully apply to AFM-based measurements in contact mode as the cantilever is subject to other forces (e.g. adhesion and capillary interaction forces) in addition to the magnetostrictive one that bends

the bimorph. We propose an extension to existing bimorph deflection analysis to account for this AFM set-up, and have obtained magnetostriction coefficients for Fe-Al thin films comparable to results achieved using other methods [36, 37].

II. MATERIALS AND METHODS

Fe-Al films with a composition of 19 at.% aluminium were deposited on Si(100) substrates and Si AFM cantilevers (Nanosensors, Pointprobes, 445 μm length, 50 μm width, 2 μm thickness, $\approx$ 0.3 N/m nominal value of elastic constant) in a multi-target dc-magnetron sputtering setup. Both Si substrates and cantilevers were supported on a turntable which rotated at 4 rpm in front of the targets, with a target - substrate distance of 35 mm. Two magnets attached to the turntable provided a permanent magnetic bias field (950 Oe) to induce uniaxial magnetic anisotropy in the deposited film, with the hard axis along the cantilever length. The substrates were cleaned prior to film deposition in ultrasonic baths of acetone and isopropyl alcohol for 10 min. In the sputtering chamber, a base pressure less than 10^{-7} Pa was established after a bake-out. The rectangular (55 x 35 x 1 mm) targets were pre-sputtered for 8 minutes for removal of oxidation layers and additional cleaning. They were run at 60 W for iron (99.5 % purity) and 23.5 W for aluminium (99.999 % purity), with the substrates at ambient temperature in 1.2 Pa Ar (99.9999 %). The film growth rate, determined by measurement of step height (Veeco Dektak 6M profilometer) at the edge of a masked region, was 0.16 nm s^{-1}. The deposition pressure was optimised to achieve minimal as-deposited stress in the films (monitored by curvature of a Kapton substrate). Phase analysis was conducted on a Bruker D8 advance X-ray diffraction system with CuKα radiation in divergent beam Bragg-Brentano geometry, showing that the films are polycrystalline, consisting of an Fe bcc structure with Al in solid solution. The film composition was quantified on a Bruker XFlash 6 EDX system within a FEI NovaNano 450 SEM. All deposited samples are assumed to be homogeneous in composition and thickness, according to previous experience, absence of peaks in X-ray diffractograms indicating the presence of difference or segregated phases, and repeatability of the measured magnetic properties on different test samples.

A PMC MicroMag 2900 Alternating Gradient Field Magnetometer has been used for characterisation of magnetic hysteresis and anisotropy of the films deposited on the Si sub-

strates. A representative $Fe_{81}Al_{19}$ (at.%) film with a thickness of 277 nm has been selected for illustrating all reported measurements. The AFM is a Bruker Multimode V Nanoscope 8 equipped with a non-magnetic scanner and head, operating under an applied magnetic field provided by a custom electromagnet, capable of generating fields up to 1000 Oe in the sample plane. Figure S1 of the supplemental material reports a schematic representation of the experimental setup. Magnetostriction measurements with the AFM have been conducted at room temperature in air.

III. RESULTS

The principle of operation of the technique consists in measuring the deflection force of a cantilever induced by a magnetostrictive film coating under an applied magnetic field. In this setup, an AFM cantilever is coated with a magnetostrictive film deposited onto the tip side of the cantilever such as represented in Figure S2 of the supplemental material. The resulting bimorph is mounted in the atomic force microscope in the standard way, and the tip approached to a non-magnetic flat and hard sample surface (Silicon oxide wafer in our case).

The microscope is operated in contact mode, and the scan size set to zero (point contact measurement), or to a small scan size (1 nm in our case). The slow scan axis is disabled, to ensure that the tip permanently remains in the same position and artefacts do not appear originating from imperfections in the sample surface or from lack of planarity. A small positive deflection setpoint must be configured for the experiment, which will cause the microscope to apply a certain force to the sample through the tip by slightly bending the cantilever. It is important to highlight that the cantilever must be mechanically "soft" and the sample surface mechanically "hard", in order to ensure that, whatever the deflection setpoint value, this induces a negligible deformation of the surface where the tip is pushing. A schematic representation of how the measurement technique works is depicted in Figure 1.

In Figure 1(a), the initial configuration at zero magnetic field is displayed. The coated cantilever bimorph is not deflected (apart from the small initial deflection discussed above, and not represented in the figure), and the tip is in contact with the flat surface of the sample. During normal operation of the microscope, its electronics will actuate the relative

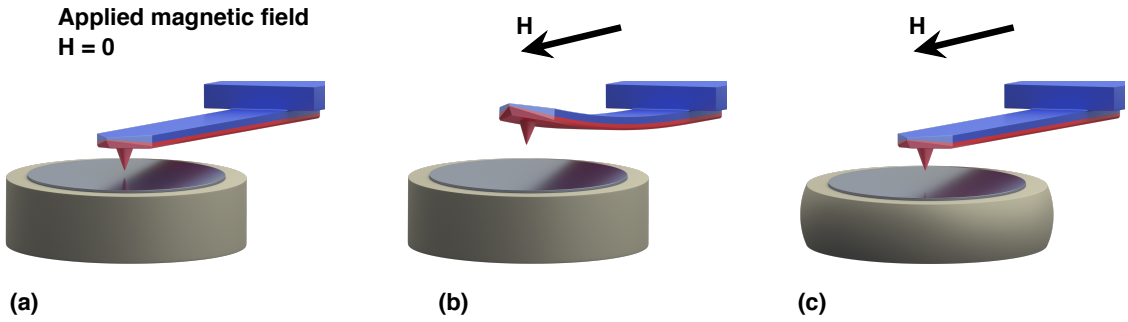

FIG. 1. Working scheme of the setup. (a) At $H = 0$, the cantilever (blue) coated with the magnetostrictive film (red) is straight; the tip is engaged to the sample surface (the light blue disk), and the AFM piezoelectric scanner (grey) is in its default position. (b) At $H > 0$, the bimorph bends upward. (c) The AFM feedback causes the piezoelectric scanner to retract, until the cantilever is straight again, keeping the deflection point constant. The representation is not in scale and the increased tip-sample distance is exaggerated.

vertical displacement of the sample through the piezo scanner with respect to the tip in order to keep the cantilever deflection constant, at the desired setpoint. As the scan area is zero, or very small, acquired images should be perfectly flat surfaces, apart from instrument or environment noise. Real-time and off-line line corrections should be disabled to improve data visualisation during the experiment.

The end-of-line signal of the microscope controller is utilised to synchronise the power supply that drives the electromagnet surrounding the microscope head. Each time a line, consisting of several hundred points (e.g. 512), has been acquired by the microscope, the power supply will change the current intensity that flows through the magnet coils; the desired field scan can be programmed, for example from positive to negative saturation and back, in any number of steps that fits within the number of lines that is used to acquire a single image with the AFM. Therefore, even if the scan area is zero or very small, the acquired AFM image must contain as many points and lines as required to accomodate all the programmed field values.

During the measurement, the applied magnetic field will induce a magnetostrictive upward deflection of the cantilever, as schematically represented in Figure 1(b). For the AFM, this is as if the tip had encountered a feature on the sample surface that has caused the cantilever to move up. This point is only a transient: as the upward curvature of the can-

tilever is interpreted by the AFM as a stronger repulsive (pushing) force, due to a feature on the sample surface, the feedback loop of the microscope will immediately react to keep the deflection setpoint constant. It will retract the sample from the tip, in order to compensate for the cantilever deflection. Assuming that there is an attractive force with a sufficiently long range, the retracted sample will attract the tip and eventually restore the initial deflection of the cantilever, as represented in Figure 1(c). This configuration corresponds to an increased tip-sample distance, that is equal to the vertical displacement Δ, performed by the piezoelectric z-stage contraction, of the sample which has moved away from the tip. The measured Δ is not equal to the deflection of a free-standing cantilever, as it is a balance between the magnetostrictive forces and the attractive ones obtained at the desired deflection setpoint. Nonetheless, the displacement Δ directly scales with the film magnetostriction.

It should be noted that the schematic representation of the principle of operation depicted in Figure 1 represents steps with finite deflections and displacements occurring in different times, whereas the process is continuous and simultaneous.

It is also important to remark that the upward deflection of the cantilever upon application of a magnetic field is achieved by depositing the film on the tip side of the cantilever for positive magnetostrictive materials, and on the back side for negative magnetostrictive ones. An inevitable increase of the tip radius by film coating and consequent degradation of horizontal resolution are irrelevant for the quality of results as measurements are performed in zero or very small scan area. The upward cantilever deflection is required, as a downward one would only increase the force exerted by the tip on the sample without resulting in a cantilever bending, being the flat surface scanned by the tip "infinitely" hard. Therefore, a proper choice of the side of the cantilever on which the magnetostrictive coating is deposited is required.

It is also necessary to acknowledge that, in principle, the proposed measurement technique could be simplified, by operating the microscope in non-contact configuration, but without cantilever oscillation. The bimorph deflection under the application of the magnetic field would directly result in a signal from the 4-quadrant photodiode of the microscope, that could be acquired, and would provide a direct measurement of the deflection of the cantilever after suitable calibration. In our tests, this method, although much simpler, turned out to be more affected by noise and less repeatable, therefore leading to the presently discussed operation of the microscope.

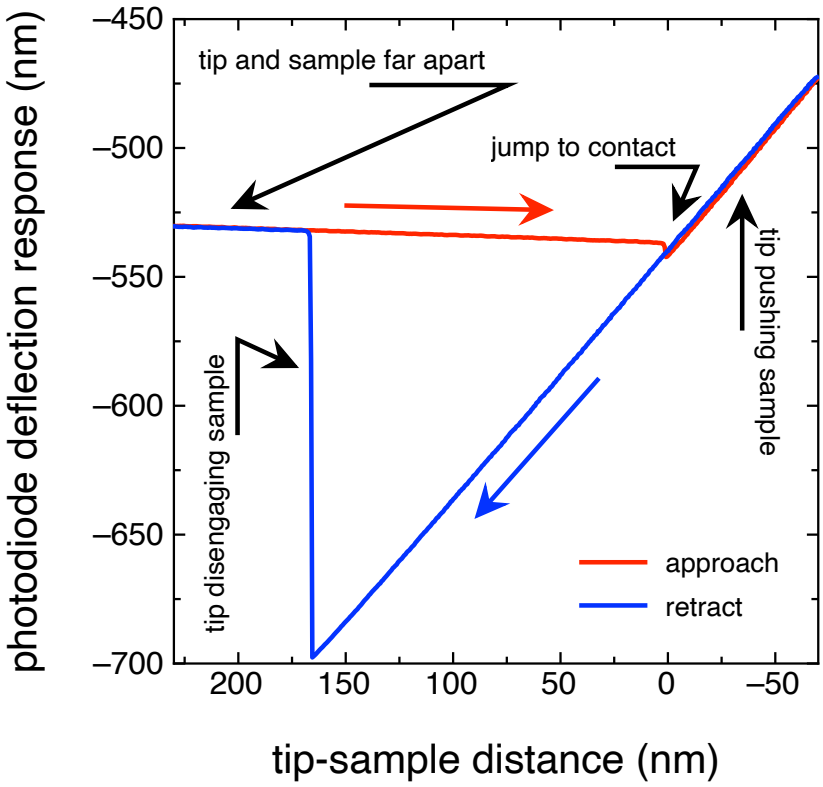

FIG. 2. Force curve acquired in air on a cantilever coated with a 277 nm thick $Fe_{81}Al_{19}$ magnetostrictive film, at zero applied magnetic field. The red curve represents the approach, from large tip-sample distance to jump-to-contact and pushing on the surface; the blue curve represents the inverse (retract) process, until the tip is disengaged from the surface and the far-distance, non-interacting behaviour is restored. The origin of the x axis is at the jump-to-contact distance. The y axis represents the AFM photodiode deflection response, in nanometers.

For the technique to work, it is necessary that a long-range attractive force keeps the tip in interaction with the scanned surface, so that when the sample is moved far away from the tip, this attractive force is able to bring the cantilever back to its original curvature, compensating the upward bending caused by magnetostriction. In order to prove that such a force actually exists, force curves [38] have been measured on all the studied bimorphs, a representative example being reported in Figure 2.

The approach curve (red line) in Figure 2 is a typical force curve where the tip-sample interaction is negligible (almost horizontal behaviour, starting from an arbitrary position where the tip and the scanned surface are very far apart). When the tip approaches the

sample surface, it eventually enters in interaction with the sample surface, in close vicinity to it, displaying the so-called jump-to-contact discontinuity, that we have used as origin of the tip-sample distance axis in Figure 2. As this distance is further reduced, the cantilever bends upwards (increase of the photodiode deflection response), since the tip is already in contact with the sample surface, that is, as previously stated, much harder than the cantilever. The relative tip-sample surface movement is then reversed, so that their distance is increased (blue curve). The zero-distance is crossed, but the tip remains in interaction with the sample surface, resulting in a downward bending of the cantilever over a tip-sample distance of ≈ 165 nm. At this point, the tip disengages the sample surface, and the deflection measured by the AFM photodiode goes back (by ≈ 170 nm) to its original value, indicating that the tip and the sample surface are no longer interacting.

The force curve shown in Figure 2, representative of all the coated cantilevers that have been measured, is characterised by a large hysteresis between the jump-to-contact and the disengagement points ($\approx$ 165 nm as stated above), due to a long-range attractive force responsible for a deflection of the cantilever of almost 170 nm. Such a force cannot be attributed to the attractive regime of the Lennard-Jones potential commonly used to model the tip-sample interactions in atomic force microscopes (which is effective only at very small distances), but is nonetheless quite common in AFM experiments performed in air, where both adhesion and capillary forces (exerted by humidity) are expected to play significant roles [39–42].

Representative images acquired with the AFM are reported in Figure 3. The microscope acquires two channels, one with the input from the Hall sensor, therefore containing the applied magnetic field values, and the other with the height values, i.e. the vertical displacement of the scanner that, as discussed above, is attributed to the vertical displacement Δ of the sample. Each image consists of 512 horizontal points in a line corresponding to single measurements that are then averaged in order to reduce the signal noise caused by the environment and feedback gains. For each row, a different magnetic field is applied. The data are interpreted as if a profile across the rows were traced (dashed line in Figure 3). For each row, the value of the signal, averaged over the acquired number of points, is extracted, and the evolution of the applied magnetic field and of the cantilever displacement as a function of the row number are obtained (panels (a) and (b)). These two sets of data can be correlated through their common parameter, the row number (the two images are

acquired at the same time), and a typical displacement *vs.* applied field curve is obtained (see Figure 3(c)). It is important to remark that, even if the scan area is zero or very small, drifts of the piezoelectric scanner may occur during the measurement. Horizontal ones are negligible, unless some feature on the scanned surface is encountered (e.g. some dirt), in which case the measurement will of course need to be repeated, because any deviation from a flat surface will affect the measured cantilever deflection. Vertical drifts, instead, if present, can be compensated by ensuring that the first and last measure points are both at the same applied field (e.g. positive saturation), and imposing that the measured deflection is the same. A linear drift with time is then assumed to correct the measured values. In our experiments, such a correction has sometimes been necessary.

A cantilever displacement curve is shown as a function of the applied field in Figure 4. The displacement curve is compared on the same field axis with the hysteresis loop measured on the corresponding film deposited on the Si substrate; it can clearly be seen that the deflection peak corresponds to the coercive field, and that the deflection curve saturates at the same field values where the hysteresis curve is also almost saturated. As a counterproof, similar experiments have been conducted on an identical uncoated cantilever, and on another commercial MFM cantilever (Bruker, MESP-HR, 225 μm length, 28 μm width, 3 μm thickness, 3 N/m nominal value of elastic constant), showing no dependence on the applied magnetic field (red line and symbols in Figure 4).

The deflection setpoint in the contact mode experiment determines the initial force at zero field that the tip exerts on the sample surface. Figure 4(b) shows Δ measured with the described technique at the saturation field for different values of the deflection setpoint. It can be seen that the maximum displacement induced by the magnetostrictive effect on the cantilever, and measured with this technique, does not depend on the deflection setpoint. This is true for all studied bimorphs, with different thickness of the magnetostrictive coating. Additionally, there is no influence on the whole deflection vs. field curve of the deflection setpoint. This confirms the robustness of the technique, and supports the approximation of the measured Δ as the result of a compensation of two opposite forces (upward deflection of the cantilever due to magnetostriction, and downward deflection of the cantilever due to attractive adhesion and capillary forces), to the deflection of a free-standing bimorph cantilever subject to a change of length of its magnetostrictive coating.

Magnetic film anisotropy has been tailored in order to guarantee maximum magnetostric-

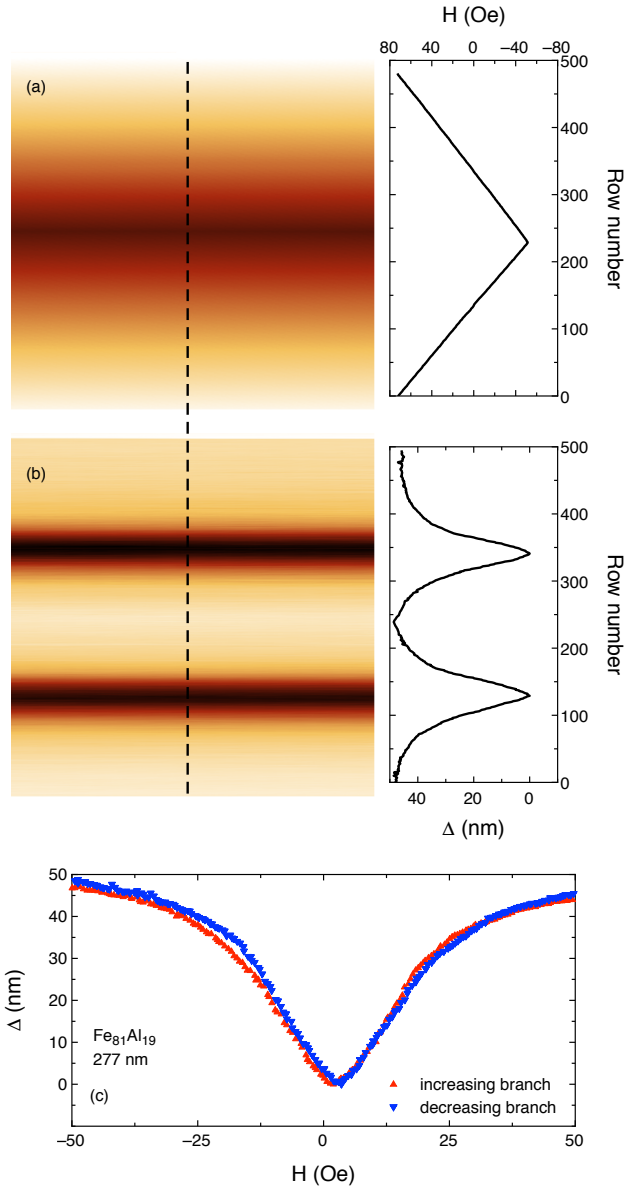

FIG. 3. (a) Image from the channel reporting the magnetic field, acquired as a function of the line row number. The corresponding values are reported in the graph, along a profile across the rows (dashed line). (b) Image of the channel reporting the height values, acquired as a function of the line row number. The corresponding values are reported in the graph, along a profile across the rows (dashed line). (c) Combination of the data reported in (a) and (b) through the common parameter row number: displacement of the cantilever as a function of the applied magnetic field, for the increasing (red symbols) and the decreasing (blue symbols) branches.

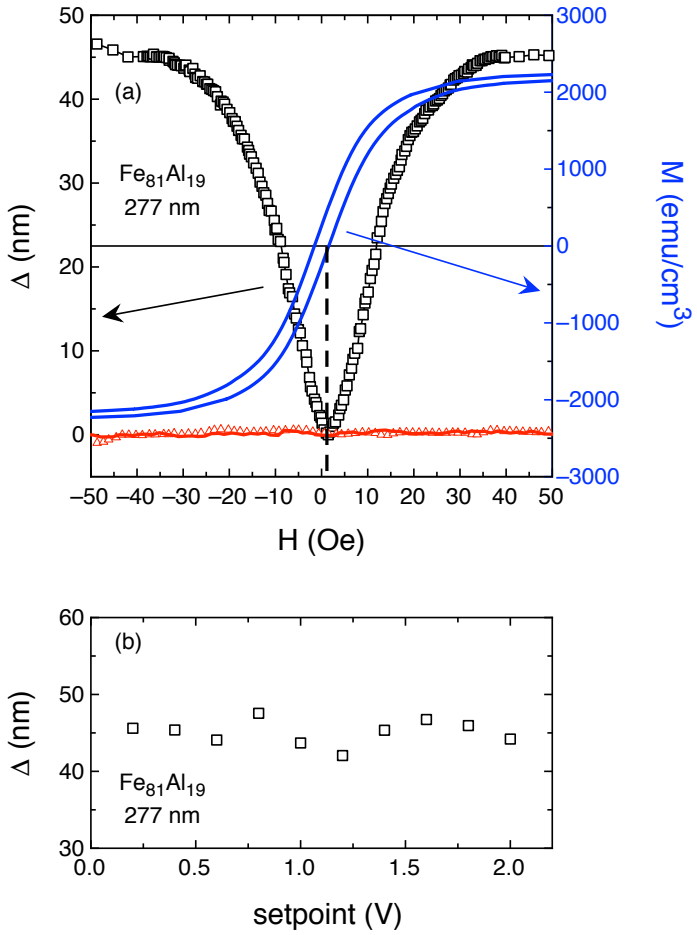

FIG. 4. (a) Vertical displacement of the piezolelectric scanner Δ as a function of the applied magnetic field for a cantilever with a 277 nm thick $Fe_{81}Al_{19}$ coating (open symbols). The corresponding hysteresis loop of the same thin films is reported as a continuous blue line. A dashed line shows the correspondence between the peak of the deflection curve and the coercive field of the loop. For comparison, an uncoated cantilever (red line) and a standard MFM cantilever (MESP-HR) (red symbols) are reported as well. (b) Δ (at the saturation field) as a function of the setpoint value for the 277 nm thick sample.

tive response. In Figure S3 of the supplemental material the angular dependence of the normalised in-plane remanence of the representative film deposited onto a Si substrate is reported. A well-developed uniaxial anisotropy lying in the film plane is clearly induced. In order to maximise the magnetostrictive response of the films, the cantilevers were oriented with their long axis perpendicular to the applied magnetic bias field direction during film

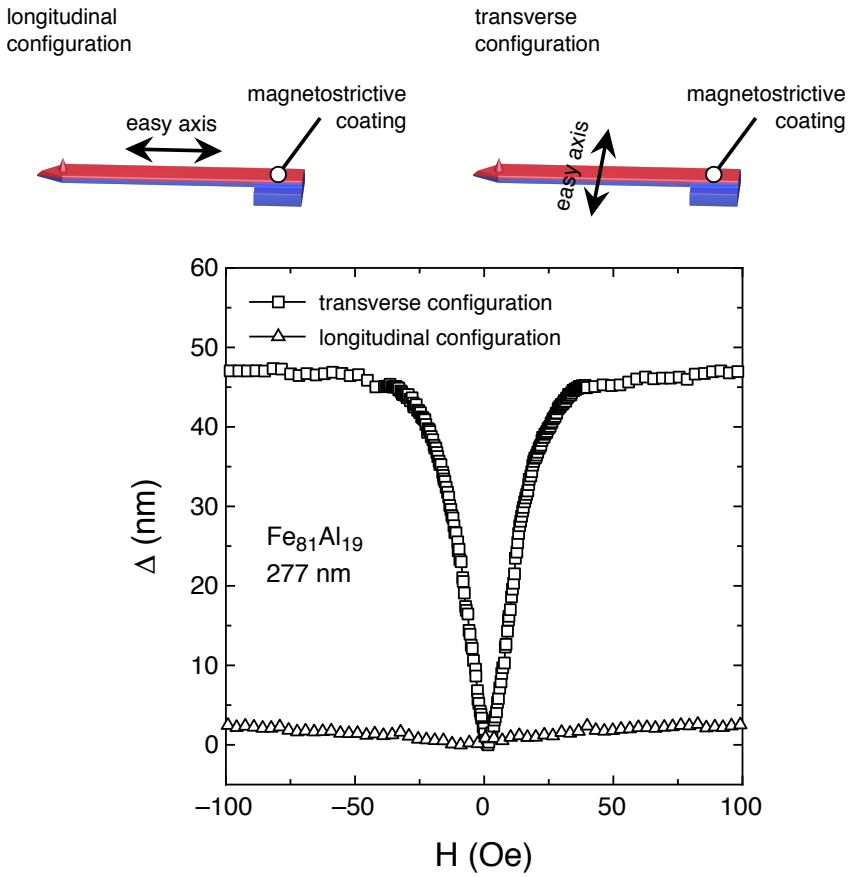

FIG. 5. Longitudinal and transverse configurations of the magnetic anisotropy with respect to the cantilever length. The graph reports the displacement of the bimorph as a function of the applied magnetic field in the longitudinal (triangles) and transverse (squares) configuration.

deposition, inducing the films' magnetic hard axis parallel to the cantilever length; this configuration is called "transverse" in Figure 5, whereas the "longitudinal" configuration deals with magnetisation processes along the cantilever length involving specimens with the magnetic easy axis aligned in the same direction. As shown in Figure 5, the magnetostrictive response is quite evident in the transverse configuration, where significant magnetisation rotation takes place upon application of the magnetic field, whereas a much smaller response is obtained when the easy axis lies along the direction of the applied field, as expected.

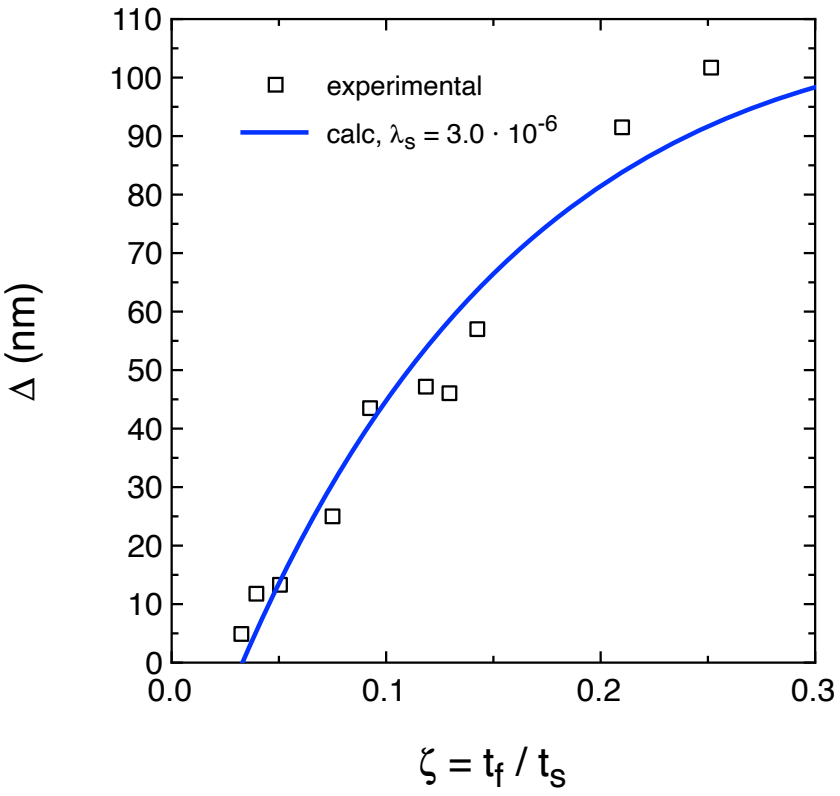

FIG. 6. Maximum cantilever displacement versus film thickness, expressed as $\zeta = {}^{t_f}/_{t_s}$ where t_f is the film thickness and t_s is the cantilever thickness (2 μm). Square symbols mark the experimental data. The blue line is the fit performed according to eq. 6.

IV. DISCUSSION

An analysis of the amplitude of the maximum displacement Δ as a function of the thickness t_f of the magnetostrictive coating on the cantilever is reported in Figure 6, through the ratio $\zeta = {}^{t_f}/_{t_s}$ where t_s is the thickness of the cantilever. A displacement equal to zero is obtained for $\zeta = 0.025$, corresponding to $t_f = 50$ nm, which deviates from the intuitive assumption that a non-zero actual deflection or bending of the cantilever should be obtained for any non-zero magnetostrictive coating thickness.

The cantilever is indeed subject to multiple distinct forces. One is of magnetostrictive origin, and is due to the elongation of the metal layer of the bimorph, inducing the upward bending of the cantilever. The deflection of such a system can be expressed according to the following equation [43]:

$$\Delta_{ms} = \frac{3\lambda_s (1+\zeta)}{\frac{1}{\chi\zeta} + 4(1+\zeta^2) + \chi\zeta^3 + 6\zeta} \frac{L^2}{t_s} \tag{1}$$

where the ms subscript refers to the magnetostrictive contribution, λ_s is the saturation magnetostriction coefficient, $\zeta = {}^{t_f}/_{t_s}$ is the ratio between the magnetostrictive coating and the cantilever thickness, L is the cantilever length, and χ is equal to:

$$\chi = \frac{\frac{E_f}{1-\nu_f^2}}{\frac{E_s}{1-\nu_s^2}} \tag{2}$$

with E being the Young modulus, and ν the Poisson ratio, and f and s suffixes referring to the metal film and substrate (cantilever) respectively. Another force acting on the cantilever is of elastic origin, that opposes any deflection, trying to restore the straight configuration of the cantilever, and is due to its elastic constant. Then, opposing any upward deflection, there are the adhesion and capillary forces discussed previously (see Figure 2), that keep the AFM tip engaged with the sample for a long range. These forces act on the free end of the cantilever and are directed downward. The other end of the cantilever is instead subject to a rigid constraint. Under these assumptions, the deflection of a beam subject to a force P acting on its free end is equal to [44]:

$$\Delta_r = \frac{1}{3}\frac{PL^3}{E_s I} \tag{3}$$

with L and E_s having the same meaning as above, and $I = \frac{wt_s^3}{12}$ where w is the cantilever width and t_s is its thickness. The r suffix refers to the "recall" nature of this contribution. In equation 3, the contribution of the metallic coating to the mechanical deflection of the cantilever has been neglected, assuming that its reduced thickness with respect to t_s would be negligible. The force P acting at the end of the cantilever is therefore the sum of two components: an elastic one, depending linearly with the tip-sample distance, that combines the elastic recall force of the cantilever and the long-range capillary forces, and a constant one, representing an adhesive force whose threshold must be overcome to start appreciating a deflection of the cantilever induced by the applied field by means of the magnetostrictive actuation. This force is necessary for taking into account the $\zeta = 0.025$ limit discussed above. The force P can therefore be expressed according to the following equation:

$$P = -P_0 - k_r d_{ts} \tag{4}$$

parameter	**value**	**notes**
E_f	$2 \cdot 10^{11}$ N/m^2	representative value for a metal
E_s	$1.7 \cdot 10^{11}$ N/m^2	representative value for Si
ν_f	0.3	representative value for a metal
ν_s	0.25	representative value for Si

TABLE I. Values of the parameters appearing in equation 6.

P_0 is the adhesion force, k_r is an effective elastic constant related to the cantilever and the capillary forces, and d_{ts} is the tip-sample distance. As discussed while describing the operation principles of the technique, the tip-sample distance is in fact Δ, the vertical displacement measured by the microscope under the application of the magnetic field, which is given by:

$$\Delta = \Delta_{ms} + \Delta_r \tag{5}$$

By substituting and rearranging the terms, the displacement Δ measured by the AFM is therefore:

$$\Delta = \frac{E_s w t_s^3}{E_s w t_s^3 + 4 k_r L^3} \left[\frac{3\lambda_s (1+\zeta)}{\frac{1}{\chi\zeta} + 4(1+\zeta^2) + \chi\zeta^3 + 6\zeta} \frac{L^2}{t_s} - \frac{4L^3 P_0}{E_s w t^3} \right] \tag{6}$$

Equation 6 can be used to fit the experimental data reported in Figure 6, keeping λ_s, P_0 and k_r as free parameters. The other parameters have the values reported in Table I, that give a value of $\chi = 1.22$.

As a result of the fitting procedure, the adhesive force P_0 has an intensity of $6.13 \cdot 10^{-9}$ N; the fitting results are weakly dependent on the recall elastic constant k_r, that can be of the order of unity and that can fluctuate above or below by an order of magnitude without significantly affecting the results ($k_r = 1$ N/m in our fit), and the saturation magnetostriction coefficient λ_s assumes a value of approximately $3.0 \cdot 10^{-6}$. This value is of the expected order of magnitude for bulk Fe-Al alloys [45]. The thin film value is slightly smaller than often reported in Fe-Al alloys, because the material is polycrystalline. Moreover, strong dependency of thin film morphology on deposition parameters may have further impact due to density fluctuations and grain structure [46].

The quality of the fitting reported in Figure 6 could be improved if the fitting equation 6

were more linear in our range of ζ values. The excessive non linearity comes from equation 1, which may not perfectly model the behaviour of a bimorph bending under the magnetostriction effect of one of its layers (see [43, 47]). Even if a more detailed equation replacing (1) would improve the fitting quality of the experimental data in Figure 6, the fitting obtained with equation 6 is nonetheless quite satisfactory, as it accounts for the finite value of ζ (and therefore of t_f) at which the displacement becomes zero, and it provides a reasonable value for λ_s.

Finally, it is worth remarking that in all the measured cases, reported in Figure 6, the maximum values of Δ are always smaller than the deflection jump of the cantilever when disengagement takes place (see Figure 2); therefore, even if the magnetostrictive effect pulls the tip away from the sample, the long-range attractive forces are still strong enough to ensure that the tip does not disengage. Should that happen, a stiffer cantilever would be required, to reduce the bending induced by the elongation of the magnetostrictive coating.

V. CONCLUSIONS

We have developed a sensitive AFM-based technique for the measurement of magnetostrictive properties of thin films. Stepwise application of a magnetic field allows the recording of reproducible magnetostrictive displacement curves with very fine field resolution. Analysis of the resulting bending forces of film-coated micro-cantilevers enables an estimation of the film magnetostriction coefficient. This technique benefits from a simple set-up, using widely available commercial components, and can be applied to a broad range of film materials and film thicknesses.

ACKNOWLEDGEMENTS

This study has been carried out and financed in the framework of the European training network project SELECTA (ETN 642642).

The Authors would like to thank Dr. Lorenzo Perolini for the fruitful discussion.

REFERENCES

[1] Ekreem, N.B.; Olabi, A.G.; Prescott, T.; Rafferty, A.; Hashmi, M.S.J. An overview of magnetostriction, its use and methods to measure these properties, *J. Mater. Process. Tech.* **2005**, *191*, 96-101.

[2] Erenstein, W.; Mathur, N.D.; Scott, J.F.; Scott, J.F. Multiferroic and magnetoelectrtic materials, *Nature* **2006**, *442759*, 759-765.

[3] Jia, Y.; Luo, H.; Zhao, X.; Wang, F. Giant magnetoelectric response from a piezoelectric/magnetostrictive laminated composite combined with a piezoelectric transformer, *Adv. Mater.* **2008**, *20(24)*, 4776-4779.

[4] Kim, Y.; Kim, Y.Y. A novel Terfenol-D transducer for guided-wave inspection of a rotating shaft, *Sensors and Actuators A Phys.* **2007**, *133(2)*, 447-456.

[5] Seco, F.; Martin, J.M.; Jimenez, A.R. Improving the accuracy of magnetostrictive linear position sensors, *IEEE Trans. Instrum. Meas.* **2009**, *58(3)*, 722-729.

[6] Hristoforou, E.; Ktena, A. Magnetostriction and magnetostrictive materials for sensing applications, *J. Magn. Magn. Mater.* **2007**, *316*, 372-378.

[7] Degen, C.L.; Poggio, M.; Mamin, H.J.; Rettner, C.T.; Rugar, D. Nanoscale magnetic resonance imaging, *PNAS* **2009**, *106*, 1313.

[8] Eom, K.; Park, H.S.; Yoon, D.S.; Kwon, T. Nanomechanical resonators and their applications in biological/chemical detection: nanomechanics principles, *Phys. Rep.* **2011**, *503(4-5)*, 115-163.

[9] Boisen, A.; Dohn, S.; Keller, S.S.; Schmid, S.; Tenje, M. Cantilever-like micromechanical sensors, *Rep. Prog. Phys.* **2011**, *74*, 036101.

[10] Arlett, J.L.; Myers, E.B.; Roukes, M.L. Comparative advantages of mechanical biosensors, *Nat. Nanotechnol.* **2011**, *6*, 203-215.

[11] Moser, J.; Güttinger, J.; Eichler, A.; Esplandiu, M.J.; Liu, D.E.; Dykman, M.I.; Bachtold, A. Ultrasensitive force detection with a nanotube mechanical resonator, *Nat. Nanotechnol.* **2013**, *8*, 493-496.

[12] Mukhopadhyay, R.; Lorentzen, M.; Kjems, J.; Besenbacher, F. Nanomechanical sensing of

DNA sequences using piezoresistive cantilevers, *Langmuir* **2005**, *21*, 8400-8408.

[13] Chaste, J.; Eichler, A.; Moser, J.; Ceballos, G.; Rurali, R.; Bachtold, A. A nanomechanical mass sensor with yoctogram resolution, *Nat. Nanotechnol.* **2012**, *7*, 301-304.

[14] Lang, H.P.; Baller, M.K.; Berger, R.; Gerber, Ch.; Gimzewski, J.K.; Battiston, F.M.; Fornaro, P.; Ramseyer, J.P.; Meyer, E.; Güntherodt, H.J. An artificial nose based on a micromechanical cantilever array, *An. Chim. Acta* **1999**, *393*, 59-65.

[15] Yango, A.; Schäpe, J.; Rianna, C.; Doschke, H.; Radmacher, M. Measuring the viscoelastic creep of soft samples by step response AFM, *Soft Matter* **2016**, *12*, 8297-8306.

[16] Schmid, S.; Jensen, K.D.; Nielsen, K.H.; Boisen, A. Damping mechanisms in high-Q micro and nanomechanical string resonators, *Phys. Rev. B* **2011**, *84*, 165307.

[17] Karablin, R.B.; Villanueva, L.G.; Matheny, M.H.; Sader, J.E.; Roukes, M.L. Stress-induced variations in the stiffness of micro- and nanocantilever beams, *Phys. Rev. Lett.* **2012**, *108*, 236101.

[18] Faust, T.; Rieger, J.; Seitner, M.J.; Kotthaus, J.P.; Weig, E.M. Signatures of two-level defects in the temperature-dependent damping of nanomechanical silicon nitride resonators, *Phys. Rev. B* **2014**, *89*, 100102(R).

[19] Yo, B.; Na, S.-M.; Flatau, A.B.; Pines, D.J. Directional magnetostrictive patch transducer based on Galfenol's anisotropic magnetostriction feature, *Smart Mater. Struct.* **2014**, *23(9)*, 095035.

[20] Squire, P.T. Magnetomechanical measurements of magnetically soft amorphous materials, *Meas. Sci. Technol.* **1994**, *5*, 67-81.

[21] Yamasaki, J.; Ohkubo, Y.; Humphrey, F.B. Magnetostriction measurement of amorphous wires by means of small-angle magnetization rotation, *J. Appl. Phys.* **1990**, *67*, 5472-5474.

[22] Siemko, A.; Lachowicz, H. On indirect measurements of saturation magnetostriction in low-magnetostrictive metallic glasses, *IEEE Trans. Magn.* **1987**, *23(5)*, 2563-2565.

[23] Gueye, M.; Zighem, F.; Belmeguenai, M.; Gabor, M.S.; Tiusan, C.; Faurie, D. Spectroscopic investigation of elastic and magnetoelastic properties of CoFeB thin films, *J. Phys. D: Appl, Phys.* **2016**, *49(14)*, 145003.

[24] Klokholm, E. The measurement of magnetostriction in ferromagnetic thin films, *IEEE Trans. Magn.* **1976**, *6*, 819-821.

[25] Weber, M.; Koch, R.; Rieder, K.H. UHV cantilever beam technique for quantitative mea-

surements of magnetization, magnetostriction, and intrinsic stress of ultrathin magnetic fims, *Phys. Rev. Lett.* **1994**, *73(8)*, 1166-1169.

[26] Pernpeintner, M.; Holländer, R.B.; Seitner, M.J.; Weig, E.M.; Gross, R.; Goennenwein, S.T.B.; Huebl, H. A versatile platform for magnetostriction measurements in thin films, *J. Appl. Phys.* **2016**, *119*, 093901.

[27] Özkale, B.; Shamsudhin, N.; Bugmann, T.; Nelson, B.J.; Pané, S. Magnetostriction in electroplated CoFe alloys, *Electrochem. Comm.* **2017**, *76*, 15-19.

[28] Tam, A.C.; Schroeder, H. Precise measurements of a magnetostriction coefficient of a thin soft-magnetic film deposited on a substrate, *J. Appl. Phys.* **1988**, *64*, 5422-5424.

[29] Jay, J.P.; Le Berre, F.; Pogossian, S.P.; Indenbom, M.V. Direct and inverse measurement of thin films magnetostriction, *J. Magn. Magn. Mater.* **2010**, *322*, 2203-2214.

[30] Papageorgopoulos, A.C.; Wang, H.; Guerrero, C.; Garcia, N. Magnetostriction measurements with atomic force microscopy: a novel approach, *J. Magn. Magn. Mater.* **2004**, *268*, 198-204.

[31] Park, J.J.; Estrine, E.C.; Reddy, S.M.; Stadler, B.J.H.; Flatau, A.B. Technique for measurement of magnetostriction in an individual nanowire using atomic force microscopy, *J. Appl. Phys.* **2014**, *115*, 17A919.

[32] Lima, B.L.S.; Maximino, F.L.; Santos, J.C.; Santos, A.D. Direct method for magnetostriction coefficient measurement based on atomic force microscope, illustrated by the example of Tb-Co film, *J. Magn. Magn. Mater.* **2015**, *395*, 336-339.

[33] Harin, E.V.; Sheftel, E.N.; Krikunov, A.I. Atomic force microscopy measurements of magnetostriction of soft-magnetic films, *Solid State Phenom. 2012*, *190*, 179-182.

[34] Penedo, M.; Fernández-Martínez, I.; Costa-Krämer, J.L.; Luna, M.; Briones, F. Magnetostriction-driven cantilevers for dynamic atomic force microscopy, *Appl. Phys. Lett.* **2009**, *95*, 143505.

[35] du Trémolet de Lacheisserie, E.; Peuzin, J.C. Magnetostriction and internal stresses in thin films: the cantilever method revisited, *J. Magn. Magn. Mater.* **1994**, *136(1-2)*, 189-196.

[36] Kawai, T.; Abe, T.; Ohtake, M.; Futamoto, M. Magnetostrictive behaviors of Fe-Al(001) single-crystal films under rotating magnetic fields, *AIP Advances* **2016**, *6*, 055931.

[37] Nakamura, S.; Morita, M.; Shinobe, K.; Matsumura, Y. Magnetostrictive characteristics of Fe-Al films formed at non equilibrium condition, *Proc. Schl. Eng. Tokai Univ., Ser.* **2008**, *E 33*, 25-28.

[38] Cappella, B.; Dietler, G. Force-distance curves by atomic force microscopy, *Surf. Sci. Rep.* **1999**, *34*, 1-104.

[39] Leite, F.L.; Bueno, C.C.; Da Róz, A.L.; Ziemath, E.C.; Oliveira Jr., O.N. Theoretical models for surface forces and adhesion and their measurement using atomic force microscopy, *Int. J. Mol. Sci.* **2012**, *13*, 12773-12856.

[40] Jang, J.; Yang, M.; Schatz, G. Microscopic origin of the humidity dependence of the adhesion force in atomic force microscopy, *J. Chem. Phys.* **2007**, *126*, 174705.

[41] Xu, W.; Blackford, B.L.; Cordes, J.G.; Jericho, M.H.; Pink, D.A.; Levadny, V.G.; Beveridge, T. Atomic force microscope measurements of long-range forces near lipid-coated surfaces in electrolytes, *Biophys. J.* **1997**, *72*, 1404-1413.

[42] Meyer, E. Atomic force microscopy, *Progress in Surface Science* **1992**, *41* 3-49.

[43] Guerrero, V.H.; Wetherhold, R.C. Magnetostrictive bending of cantilever beams and plates, *J. Appl. Phys.* **2003**, *94(10)*, 6659-6666.

[44] Viola, E. *Esercitazioni di scienza delle costruzioni*, Vol. 2, Pitagora Editrice: Bologna, Italy, 1985, p. 414.

[45] Cullen, J.R.; Clark, A.E.; Wun-Fogle, M.; Restorff, J.B.; Lograsso, T.A. Magnetoelasticity of Fe-Ga and Fe-Al alloys, *J. Magn. Magn. Mater.* **2001**, *226-230*, 948-949.

[46] Thornton, J.A. Influence of substrate temperature and deposition rate on structure of thick sputtered Cu coatings, *J. Vac. Sci. Technol.* **1975**, *12(4)*, 830-835.

[47] Dan, J.; Gibbs, M.R.J.; Schrefl, T. Finite-element analysis on cantilever beams coated with magnetostrictive material, *IEEE Trans. Magn.* **2006**, *42(2)*, 283-288.

Measurement of thin film magnetostriction using field-dependent atomic force microscopy

Marco Coïsson[1],* Wilhelm Hüttenes[2],† Matteo Cialone[3,1], Gabriele Barrera[1], Federica Celegato[1], Paola Rizzi[3], Zoe H. Barber[2], and Paola Tiberto[1]

[1] *Advanced Materials and Life Sciences Division, INRIM, Torino, Italy*

[2] *Department of Materials Science and Metallurgy, Cambridge University, UK and*

[3] *Department of Chemistry, University of Torino, Italy*

* m.coisson@inrim.it

† wkgh2@cam.ac.uk

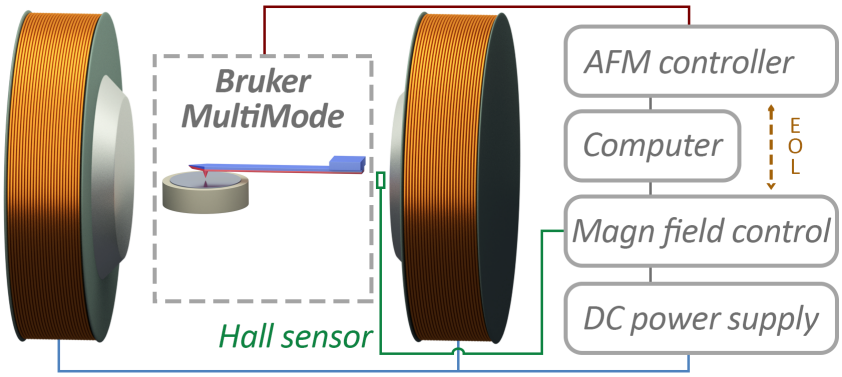

FIG. 1. Schematic representation of the experimental setup used for magnetostriction measurements. A fully non-magnetic atomic force microscope is placed in the gap of an electromagnet, providing a magnetic field parallel to the sample and to the AFM cantilever. A Hall probe measures the applied magnetic field. A magnetic field control unit uses the end-of-line signal coming from the AFM controller to synchronise the power supply that drives the electromagnet, so that each line measured by the microscope is acquired at a different applied magnetic field.

Figure S1 shows a schematic representation of the arrangement of the experimental setup used for measuring the magnetostriction. It consists of a Multimode V Nanoscope 8 Bruker AFM, with fully non-magnetic head and scanner, that are placed in the gap of an electromagnet capable of generating magnetic fields up to 1000 Oe. The magnetic field is parallel to the sample surface and to the AFM cantilever. The magnetic field is measured by a Hall probe, and the field value is fed to the AFM controller to be acquired together with the other microscope channels. The end-of-line signal of the microscope is used to trigger the DC power supply that drives the electromagnet, so that each line acquired by the AFM corresponds to a different magnetic field. The applied magnetic fields, in sequence, can build up any field history.

Figure S2 shows SEM images of an AFM cantilever after the deposition of a $Fe_{81}Al_{19}$ thin film with a thickness of 185 nm. Different magnifications are reported, showing the whole

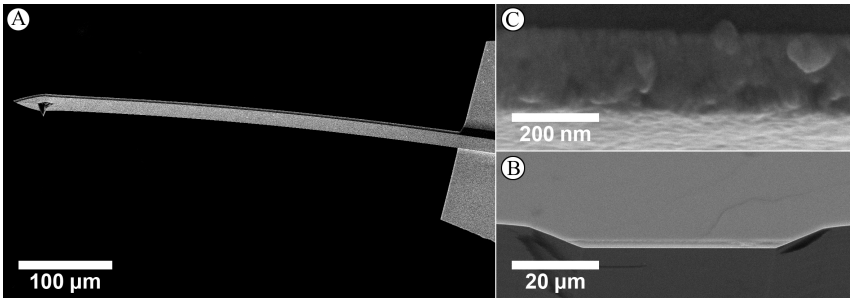

FIG. 2. (a) SEM image of an AFM cantilever after depositing a $Fe_{81}Al_{19}$ film of 185 nm. (b) SEM image of a cross section of the cantilever base. (c) SEM image in cross section of the magnetic film deposited on the cantilever (zoom in of panel (b)).

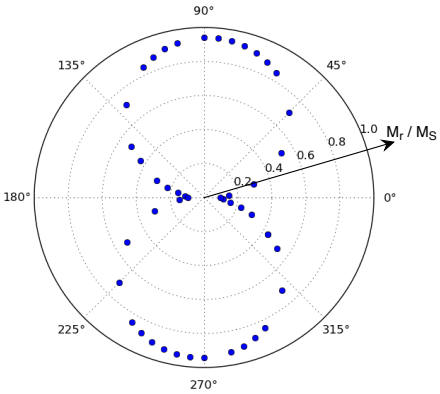

FIG. 3. Remanence to saturation ratio as a function of the angle of application of the magnetic film for a $Fe_{81}Al_{19}$ film 277 nm thick sputtered under an applied magnetic field of 950 Oe along the direction marked as 90°.

cantilever (panel (a)), the cross section of the cantilever base (panel (b)), and a cross section of the metallic film (panel (c), zoomed in from panel (b)).

Figure S3 shows the remanence to saturation ratio of a continuous $Fe_{81}Al_{19}$ thin film 277 nm thick. The measurements have been performed by applying the magnetic field along different directions in the in-plane configuration. During preparation, the film has been submitted to a magnetic field of 950 Oe aligned along the direction marked as 90°.